Coexistence of Wi-Fi and IoT Communications in WLANs

Hossein Pirayesh, Pedram Kheirkhah Sangdeh, and Huacheng Zeng

***Abstract*—As most Internet of Things (IoT) devices are powered by small-sized batteries and expected to operate for many years without battery replacement, energy-efficient wireless IoT communication has been considered as a crucial component of future network infrastructure. In this paper, we propose a practical design (termed WiFi-IoT) to add energy-efficient IoT communication capability into WLANs. WiFi-IoT features two innovative techniques: an asymmetric physical (PHY) design and a transparent coexistence scheme. The asymmetric PHY allows an access point (AP) to communicate with multiple IoT devices at a much low sampling rate (250 ksps), thereby significantly reducing the power consumption for IoT devices. The transparent coexistence scheme enables a multi-antenna AP to serve Wi-Fi and IoT devices simultaneously, leading to an efficient utilization of spectrum. We have built a prototype of WiFi-IoT on a USRP2 wireless testbed and evaluated its performance in real-world wireless environments. Experimental results show that a two-antenna AP can simultaneously serve one broadband Wi-Fi device and 24 narrow-band IoT devices on the same spectrum.**

***Index Terms*—Internet of Things, Wi-Fi networks, wireless communications, energy efficiency.**

I. Introduction

The Internet of Things (IoT) is the strategy of extending Internet connectivity beyond standard electronic devices (e.g., desktops, laptops, and smartphones) to any type of traditionally dumb physical devices and everyday objects. With the continuous driving forces from governments and industry, the number of IoT devices has reached 7.1 billion in 2018, and the IoT market is still flourishing. It is estimated that, by 2025, the number of IoT devices will reach 21.5 billion and the global IoT market value will achieve $7.1 trillion [1]. This massive number of connected devices have been used in diverse domains and areas, such as smart cities [2], smart homes [3], healthcare devices [4], industries [5], and transportation systems [6]. As most IoT devices are powered by batteries and limited by their physical size, energy-efficient wireless communication is an enabler for them to interact with the cyber-physical world. To support energy-efficient IoT communication, a number of low-power wireless technologies have been explored, such as ZigBee [7], LoWPAN [8], Bluetooth Low Energy [9], and Z-Wave [10]. These existing technologies, however, are limited to the communication for only two IoT devices in a time slot due to the lack of spatial multiplexing, and thus not suited for providing connectivity for massive IoT devices.

Recognizing this vacancy, 3GPP has developed Narrow-Band IoT (NB-IoT) to provide a wide range of cellular services for IoT devices [11]. In contrast to the legacy LTE standards that use broadband spectrum (e.g., 20 MHz) to provide high-speed services for mobile devices, NB-IoT limits its communication bandwidth to 200 kHz so as to reduce the power consumption for the IoT devices. While NB-IoT has received many successes, there are two concerns about its commercial applications. First, similar to cellular services for mobile phones, NB-IoT services will not come for free. Users have to pay recurring fee to enjoy the NB-IoT services (e.g., one dollar per month per device). Although this fee is not much compared to phone bill, it easily becomes significant if one has many IoT devices in use. The recurring fee of NB-IoT services imposes a heavy financial burden on end users. Second, cellular networks are already very crowded. Serving additional billions of IoT devices may result in traffic congestion for cellular networks, especially considering the fact that the licensed spectrum bands suitable for energy-efficient IoT communication (below 6 GHz) are depleting. These two concerns push us to explore an alternative energy-efficient IoT communication solution to complement NB-IoT.

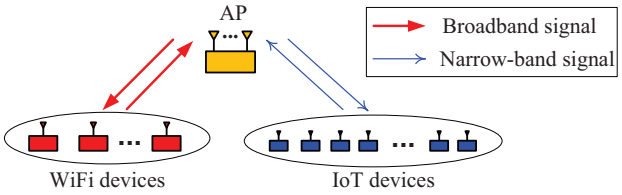

Fig. 1: A future WLAN with both Wi-Fi and IoT devices.

In this paper, we propose a practical design (termed WiFi-IoT) to add energy-efficient IoT communication capability into future WLANs, as illustrated in Fig. 1. WiFi-IoT is motivated by the following two observations. First, Wi-Fi is the dominant Internet service infrastructure in indoor environments. It also has a large outdoor coverage in urban and suburban areas. By upgrading Wi-Fi access point's (AP's) air interface, the existing Wi-Fi infrastructure can be leveraged to offer energy-efficient IoT services in many scenarios. Second, Wi-Fi has demonstrated its success as an Internet provider for mobile devices. As expected, enabling IoT communication in Wi-Fi will dramatically offload the cellular IoT traffic, thereby mitigating the traffic congestion in cellular networks. Given its potentials, a successful design of WiFi-IoT will not only address the above two concerns about NB-IoT, it will also accelerate the evolution of IoT ecosystems.

WiFi-IoT faces two challenges. The first one is to preserve the energy efficiency of IoT devices. Since most IoT devices are powered by small-sized batteries, it is imperative to minimize their power consumption in radio communications.

The authors are with the Department of Electrical and Computer Engineering, University of Louisville, Louisville, KY 40292.

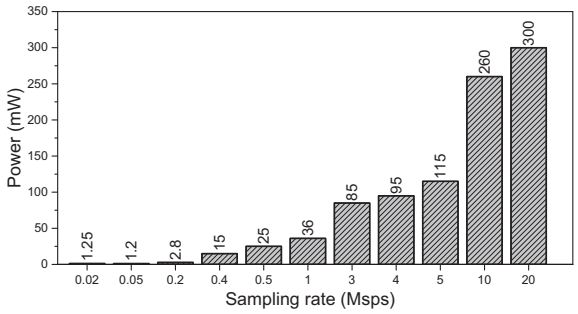

Fig. 2: Power consumption versus sampling rate of ADC in wireless communication systems [12].

Simply embedding ordinary Wi-Fi chipset into IoT devices is not a plausible solution as it consumes too much energy. To address this challenge, we propose an asymmetric PHY design, which enables an OFDM-based broadband AP to communicate with many QAM-based (non-OFDM) narrow-band IoT devices at a much low sampling rate (250 ksps).[1] The asymmetric PHY is designed based on the intrinsic properties of OFDM modulation and radio frequency mixer. The trick is that, instead of using the same carrier frequency for all IoT devices, each IoT device tunes its carrier frequency to a particular subcarrier of the AP's OFDM signal. Doing so makes it possible for an IoT device to encode and decode its baseband signal at a low sampling rate without FFT/IFFT operation. As shown in Fig. 2, the reduction of ADC sampling rate (from 20 Msps to 250 ksps) can save about 300 mW (97%) power for an IoT device. Moreover, the elimination of FFT/IFFT operation can save another 41 mW power [13]. As ADC and FFT/IFFT are two of the most power-hungry components of a wireless transceiver [14], such an asymmetric PHY will lead to a significant power reduction for IoT devices.

The second challenge is the coexistence of broadband Wi-Fi devices and narrow-band IoT devices. To harmonize their coexistence, a straightforward approach is that the AP schedules Wi-Fi and IoT devices into different time slots. Such a TDMA-based approach will avoid their mutual interference and create interference-free environments for their respective communications. However, since a considerable portion of airtime will be allocated to IoT devices, this approach tends to sacrifice the quality of service (QoS) for Wi-Fi devices. To enable transparent coexistence of Wi-Fi and IoT devices and maximize the spectral efficiency, we propose a SDMA-based approach that allows a multi-antenna AP to serve broadband Wi-Fi devices and narrow-band IoT devices simultaneously. The key component of our approach is a lightweight interference cancellation method, which can effectively mitigate the mutual interference in practice by leveraging the spatial degrees of freedom provided by AP's multiple antennas. Specifically, in the uplink, we construct a spatial linear filter at the AP to decode the signals from each individual Wi-Fi/IoT device in the presence of cross-technology interference. In contrast to existing signal detection methods such as zero-forcing (ZF) and MMSE, our method does not require channel estimation and turns out to be very robust in practice. In the downlink, we construct beamforming filters for the AP to enable concurrent data transmissions. Different from existing beamforming techniques, which require channel state information (CSI) for the construction of beamforming filters, our technique simply uses the decoding filters obtained in the uplink as the beamforming filters. The elimination of the need for CSI not only simplifies the system complexity, but it also reduces the airtime overhead induced by channel feedback. Leveraging these two interference cancellation techniques, WiFi-IoT is capable of serving Wi-Fi and IoT devices on the same spectrum simultaneously.

We have built a prototype of WiFi-IoT on a GNURadio-USRP2 wireless testbed and evaluated its performance in an office building environment. Experimental results show that, using WiFi-IoT, an AP with two antennas can serve one Wi-Fi device and 24 IoT devices simultaneously in both uplink and downlink, with each IoT device achieving more than 375 kbps. Our prototype provides a reference design to the community as an alternative solution to supporting energy-efficient IoT communication and sheds light on the integration of energy-efficient IoT communication in future Wi-Fi standards. We note that our design targets the stationary or semi-stationary environments such as smart home with smoke detection sensors, door opening sensors, or smart meters. The design of IoT communications in highly dynamic environments with frequent roaming is beyond the scope of this work.

The remainder of this paper is organized as follows. Section II surveys the related work. Sections III outlines the asymmetric PHY for IoT communication. Section IV presents a coexistence scheme for WiFi-IoT. Section V presents our experimental results and Section VI concludes the paper.

II. Related Work

To the best of our knowledge, this paper is the first one that attempts to enable the coexistence of Wi-Fi and IoT communications in WLANs. Some relevant research efforts are surveyed below.

NB-IoT in Cellular Networks: 3GPP has introduced various technologies to offer IoT communication services in cellular networks, such as NB-IoT [11], EC-GSM-IoT [15], and eMTC [16]. Among the existing IoT technologies, NB-IoT is the most promising and successful one. It uses a narrow-band channel to support a massive number of low data-rate IoT devices [17]. Different from NB-IoT, our design is to enable energy-efficient IoT communications in WLANs. Moreover, our design is focused on the coexistence of IoT and Wi-Fi communications on the same spectrum band. From the application standpoint, our design will complement NB-IoT in many scenarios.

Narrow-Band Communications in WLANs: Recently, the industry has launched efforts to develop energy-efficient narrow-band communications in WLANs. In a new amendment of 802.11ah [18], Wi-Fi Halow was introduced by Wi-Fi Alliance to provide low-power and long-range IoT communication services. It uses 2 MHz channel bandwidth and operates in 900 MHz spectrum. In the context of 802.11ax

[1]The sampling rate refers to the frequency of ADC converting analog signal to digital samples at a radio receiver.

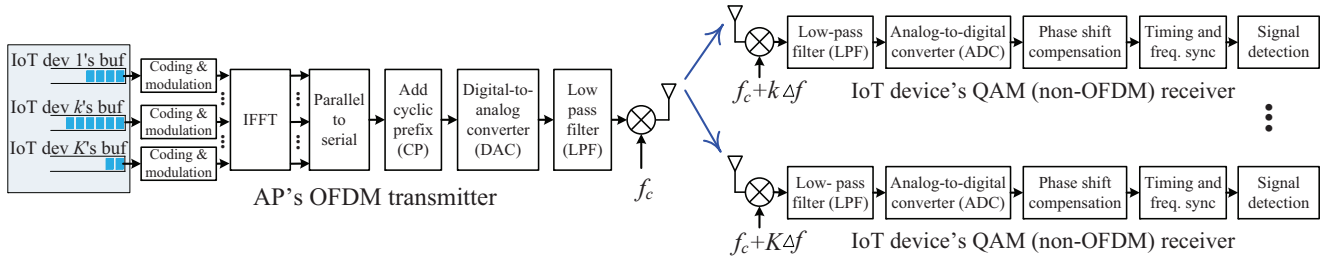

(a) Asymmetric PHY design for downlink data transmission.

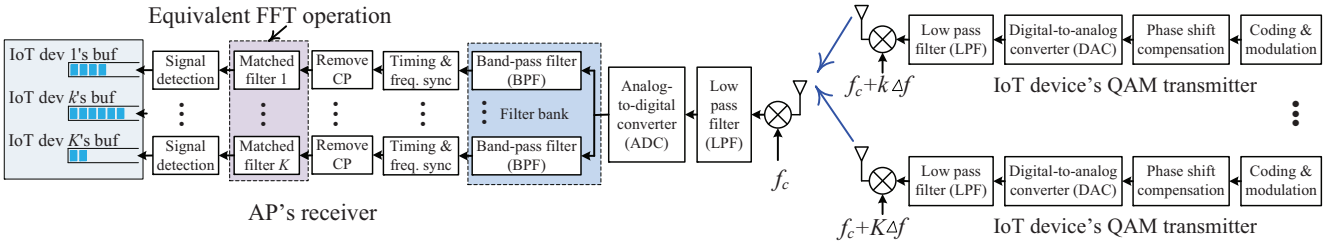

(b) Asymmetric PHY design for uplink data transmission.

Fig. 3: Asymmetric PHY design for the concurrent communications between the AP and K IoT devices.

amendment [19], small-bandwidth communication (e.g., using a single resource unit or 2 MHz) has been studied to offer IoT communication services. For example, in [20], an overlay narrow-band IoT communication approach was proposed for 802.11ax. In [21], narrow-band IoT communication in Wi-Fi networks was studied and evaluated using simulation from 802.11ax MAC protocol perspective. In [22], NB-WiFi was proposed for 802.11ax by advocating Bluetooth Low Energy (BLE) for IoT communication. Our work differs from this efforts as we use a single OFDM subcarrier for IoT communication, without the need of OFDM modulation at the IoT devices.

Coexistence of Heterogeneous Technologies: In the literature, there is a large volume of work on the coexistence of heterogeneous wireless communication systems, which is also known under the names of spectrum sharing and cognitive radio (see [23]–[25] and references therein). Most of the existing work focused on enabling concurrent spectrum utilization for heterogeneous networks with or without inter-network cooperation. While the existing work in this domain considers spectrum sharing only, our work considers not only spectrum sharing but also infrastructure sharing. As we shall see, the new-designed AP in WLANs will be able to simultaneously serve both Wi-Fi and IoT devices on the same spectrum band. Thus, our work significantly differs from the existing work.

III. IoT Communication: A Primer

In [26], we presented an asymmetric PHY design to enable the energy-efficient communication between the AP and K IoT devices. The salient features of our design include: i) each IoT device communicates with the AP using a single OFDM subcarrier; ii) the IoT devices use low sampling rate (250 ksps) for signal transmission and reception; and iii) the AP can serve many (up to 24) IoT devices simultaneously in its OFDM modulation. In what follows, we outline the PHY design for the IoT communication between the AP and the IoT devices.

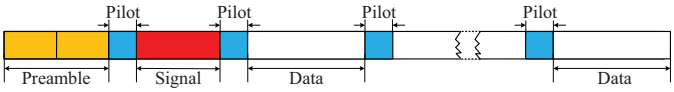

Fig. 4: Physical-layer frame format for IoT communications.

Frame Format Fig. 4 shows the frame format, which has the following four fields. i) *Preamble field:* This field is designed for synchronization and channel equalization. It consists of two identical Zadoff-Chu sequences of M_p symbols. ii) *Signal field:* This field is used to define the modulation and coding scheme (MCS) used in the data field as well as length of the frame. The MCS type of the symbols in this field is fixed. The number of symbols in this field, which we denote as M_s, can be specified by the upper layer. iii) *Pilot field:* This field is one pre-defined reference symbol, which will be used to correct phase offset for signal detection at the IoT devices. iv) *Data field:* This field is used to carry payloads. The number of symbols in this field, denoted as M_d, can be user-defined.

Downlink IoT PHY: As shown in Fig. 3(a), a new PHY was presented in [26] to support the IoT communication from an AP to K IoT devices. The key idea is that the AP uses K different OFDM subcarriers to communicate with K different IoT devices. At each IoT device, a low pass filter is applied to suppress the inter-subcarrier interference, and a sophisticated signal processing algorithm was presented to combat inter-symbol interference. Our experimental results in [26] show that this design enables an AP to send packets to 24 IoT devices simultaneously in real-world wireless environments.

Uplink IoT PHY: As shown in Fig. 3(b), a new PHY was presented in [26] to support the uplink IoT communication from K IoT devices to an AP. The key challenge is the asynchrony of the uplink signals from the IoT devices, which cannot achieve fine-grained time and frequency synchronizations in real world. To address this challenge, we presented a new PHY for the AP as shown in Fig. 3(b). Our experimental results

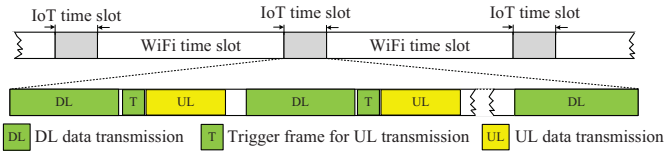

Fig. 5: Illustration of a TDMA-based protocol for the coexistence of Wi-Fi and IoT devices in WLANs.

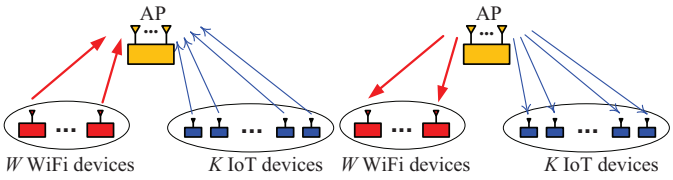

(a) Uplink transmission (b) Downlink transmission

Fig. 6: Coexistence of W Wi-Fi devices and K IoT devices in uplink and downlink. Each Wi-Fi device sends/receives broadband signals to/from the AP using OFDM modulation, whereas each IoT device sends/receives narrow-band signals to/from the AP using a single OFDM subcarrier.

have shown that this design can enable the AP to decode the packets from 24 independent IoT devices in real-world wireless environments.

IV. Coexistence of Wi-Fi and IoT Communications

In [26], we have presented a TDMA-based protocol to enable the coexistence of Wi-Fi and IoT devices. Specifically, the AP schedules Wi-Fi and IoT devices into different time slots so the mutual interference can be avoided in the time domain, as illustrated in Fig. 5. In this paper, we propose a more efficient coexistence scheme by taking advantage of the AP's multiple antennas to enable the spectrum sharing between the Wi-Fi and IoT devices in the spatial domain. Such a SDMA-based approach will allow a multi-antenna AP to serve Wi-Fi and IoT devices simultaneously, thereby improving the spectral efficiency and scheduling flexibility. It is noteworthy that this work focuses on the design of efficient solutions to enable the coexistence of Wi-Fi and IoT devices. The cross-technology interference from ZigBee, Bluetooth, or other ISM devices is not considered in our design. This type of interference can be handled by other existing designs [27]–[30].

A. Basic Idea and Overview

The principle of our coexistence scheme is similar to that of multi-user MIMO (MU-MIMO). In the uplink as shown in Fig. 6(a), the AP receives a blend of signals from all Wi-Fi and IoT devices. To decode those signals, the AP constructs a spatial filter (also called decoding filter or detection filter) that can cancel out the inter-user interference and recover the desired signal. Specifically, to decode the signals from a Wi-Fi device, the AP constructs a decoding filter for each of the subcarriers. Such a decoding filter will cancel the interference from other Wi-Fi devices and all the IoT devices. To decode the signals from an IoT device, the AP constructs a spatial filter that can cancel out the interference from all the Wi-Fi devices. Since different IoT devices use different subcarriers (radio frequencies), the signals from different IoT devices will not interfere each other.

In the downlink as shown in Fig. 6(b), to enable concurrent data transmissions, the AP pre-cancels the interference using beamforming technique on the transmitter side, so that each Wi-Fi/IoT device will receive its desired signal without any interference. For each Wi-Fi device, the AP constructs a spatial filter (also called beamforming filter) for each of its subcarriers in the OFDM modulation. Such a beamforming filter will steer the signal power to the target Wi-Fi device while nullify the signal power at other devices. Similarly, for each IoT device, the AP constructs a beamforming filter for signal precoding. This beamforming filter will steer the signal power to the target IoT device and nullify the signal at other devices. With the beamforming at the AP, the Wi-Fi and IoT devices will only receive their desired signals and therefore are capable of decoding their respective data packets in the downlink.

While the principle is straightforward, a big question is how to construct the decoding filters in the uplink and the beamforming filters in the downlink. We will answer this question shortly. Before we answer this question, we would like to offer some discussions on the proposed coexistence scheme.

Spatial Degrees of Freedom (SDoF): The proposed coexistence scheme can be interpreted using the concept of SDoF in the information theory. For the AP with M antennas, it has M SDoF, each of which can be used to support one data stream transmission for either Wi-Fi or IoT device. For the network as shown in Fig. 6, the W Wi-Fi devices will consume W SDoF at the AP, and the K IoT devices will consume one SDoF at the AP. This is because the K IoT devices use different subcarriers for data transmission and therefore occupy only one spatial direction. To ensure that the AP has enough SDoF for multi-user detection in the uplink and beamforming in the downlink, we have the following constraints: $W + 1 \leq M$. It is worth pointing out that we assume the channels between the AP and the Wi-Fi/IoT devices have full rank. If the channels are deficient in rank, then the number of Wi-Fi/IoT devices that the AP can simultaneously serve will decrease correspondingly.

Heterogeneous versus Homogeneous MU-MIMO: The proposed coexistence scheme can be regarded as a heterogeneous MU-MIMO transmission where the users are Wi-Fi and IoT devices. Compared to homogeneous (conventional) MU-MIMO, heterogeneous MU-MIMO faces two challenges in the design of decoding filters in the uplink and beamforming filters in the downlink.

First, in the uplink transmission of homogeneous MU-MIMO, the user devices are typically well synchronized in both time and frequency domain. As a result, the uplink channel between the AP and each user device can be estimated at the AP, and the estimated channel can be used to decode the signals. However, in the uplink transmission of heterogeneous MU-MIMO (see Fig. 6(a)), it is very hard to achieve the time synchronization (at the level of 50 ns) among the Wi-Fi and IoT devices, because the IoT devices operate at a much lower clock frequency. As a consequence, the AP

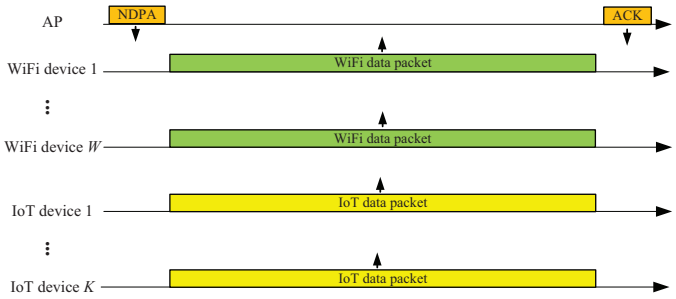

Fig. 7: Uplink MAC protocol for data transmission of coexisting Wi-Fi and IoT devices.

cannot estimate the uplink channels, which are needed for the conventional signal detection methods (e.g., ZF and MMSE). To address this challenge, we propose a channel-agnostic method for the signal detection. Unlike conventional signal detection methods that require CSI, our proposed method does not require CSI. Instead, it constructs the decoding filters for signal detection directly based on the corrupted reference signals.

Second, in the downlink transmission of heterogeneous MU-MIMO (see Fig. 6(b)), the acquisition of downlink channels for the design of beamforming filters is a costly task as it entails a large amount of airtime overhead, especially considering the MAC-level coordination for channel feedback among the Wi-Fi and IoT devices. To reduce the airtime overhead, we propose a lightweight beamforming method, which takes advantage of wireless channel reciprocity and directly uses the decoding filters in the uplink as the beamforming filters in the downlink.

B. Uplink Transmission

In this section, we first present a MAC protocol for uplink transmission, and then present the construction of decoding filters for the AP to decode the signals from the Wi-Fi and IoT devices, respectively.

Uplink MAC Protocol. Fig. 7 shows the proposed MAC protocol to enable the concurrent uplink transmissions for Wi-Fi and IoT devices. In this protocol, the AP first broadcasts an NDPA (null data packet announcement) frame to notify the Wi-Fi and IoT devices of the uplink data transmission. It contains the address of the AP and the selected devices. Upon receipt of the NDPA frame, the Wi-Fi and IoT devices send their data packets to the AP simultaneously. After the AP receives and decodes the uplink data packets, it responds with an ACK/NACK packet to inform each Wi-Fi/IoT device if its data packet has been successfully decoded. When an IoT device has no data packet for transmission, it will simply switch to the sleep mode to reduce its power consumption. The IoT device only needs to listen the beacon packets, which is broadcasted by the AP every 100 ms. Then, the AP can wake up an IoT device by setting commands in its next beacon packet. When the IoT device itself has data packets coming to its radio buffer for transmission, it will wake up and obtain the parameters for transmission by listening the beacon packets.

Decoding Wi-Fi Signal at AP. In the proposed protocol, the AP needs to decode the mixed signals from the Wi-Fi and IoT devices. To do so, we propose a heuristic signal detection method. In our method, the AP decodes the signal from each device separately. When decoding the signal from one device, it simply treats the signals from other devices as interference and constructs a spatial filter to cancel the interference and recover the desired signal by leveraging the reference signals embedded in each frame (packet). Mathematically, to decode the signal on subcarrier k from Wi-Fi device i, the AP constructs a spatial filter $\mathbf{G}_i(k) \in \mathbb{C}^{M\times 1}$ as follows:

$$\mathbf{G}_i(k)=\Big[\sum_{(l,k')\in\mathcal{R}_k}\mathbf{Y}(l,k')\mathbf{Y}(l,k')^{\mathsf{H}}\Big]^{+}\Big[\sum_{(l,k')\in\mathcal{R}_k}\mathbf{Y}(l,k')\bar{X}_i(l,k')^{\mathsf{H}}\Big], \tag{1}$$

where $\mathbf{Y}(l,k') \in \mathbb{C}^{M\times 1}$ is the AP's received frequency-domain signals in OFDM symbol l on subcarrier k', which includes the signals from all Wi-Fi and IoT devices. $\bar{X}_i(l,k')$, $(l,k') \in \mathcal{R}_k$, is the set of reference signals (e.g., L-STF and L-LTF [31]) in the frame that are used to construct subcarrier k's decoding filter. $(\cdot)^{\mathsf{H}}$ is conjugate transpose operator. $(\cdot)^{+}$ is pseudo-inverse operator. After constructing the decoding filter, the AP estimates the signals from Wi-Fi device i in the face of interference from other Wi-Fi/IoT devices by: $\hat{X}_i(l,k) = \mathbf{G}_i(k)^{\mathsf{H}}\mathbf{Y}(l,k)$, $\forall l,k$, where $\hat{X}_i(l,k)$ is the estimated signal from Wi-Fi device i.

Decoding IoT Signal at AP. A similar method has been used at the AP to decode the signal from each IoT device in the presence of interference from Wi-Fi devices. However, (1) cannot be directly used to decode IoT signals. This is because the IoT signal is not an OFDM signal, but a narrowband signal. Hence, the AP's IoT Rx-PHY does not have FFT operations. It uses matched filters to convolute the signals from each IoT device (see Fig. 3b). To decode the IoT signal, we make some minor changes in the construction of the decoding filter.

With a bit abuse of notation, we denote k as the index of IoT devices and l as the index of data symbol from the IoT device. Denote $\mathbf{y}(l,k) \in \mathbb{C}^{M\times 1}$ as the AP's received baseband signal from its IoT-Rx PHY (i.e., the output signal of the matched filters on the left-hand side of Fig. 3b). Denote $\bar{X}(l,k)$, $l \in \mathcal{L}_{\text{ref}}$, as the set of reference signals in the IoT frame (i.e., the preamble of the IoT frame in Fig. 4). Denote $\mathbf{G}(k)$ as the spatial filter constructed to decode the signal from IoT device k. Then, we construct $\mathbf{G}(k) \in \mathbb{C}^{M\times 1}$ as follows:

$$\mathbf{G}(k)=\Big[\sum_{l\in\mathcal{L}_{\text{ref}}}\mathbf{y}(l,k)\mathbf{y}(l,k)^{\mathsf{H}}\Big]^{+}\Big[\sum_{l\in\mathcal{L}_{\text{ref}}}\mathbf{y}(l,k)\bar{X}(l,k)^{\mathsf{H}}\Big]. \tag{2}$$

After constructing the decoding filter, the AP estimates the signals from IoT device k by: $\hat{X}(l,k) = \mathbf{G}(k)^{\mathsf{H}}\mathbf{y}(l,k)$, $\forall l,k$.

C. Downlink Transmission

Similar to the previous section, we first propose a MAC protocol for downlink transmission and then present the construction procedure of beamforming filters for the AP.

Downlink MAC Protocol. Fig. 8 shows the proposed MAC protocol enabling the concurrent downlink transmissions for Wi-Fi and IoT devices. The protocol has the following steps: (i) The AP first broadcasts an NDPA packet to inform the

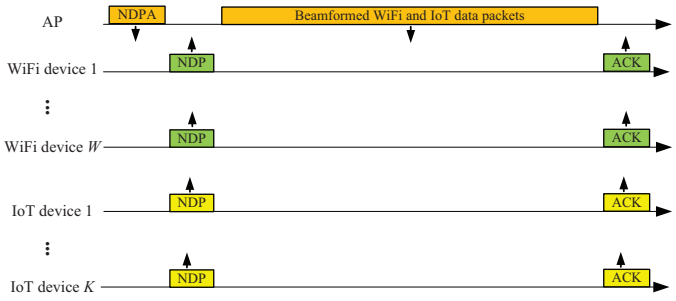

Fig. 8: Downlink MAC protocol for data transmission of coexisting Wi-Fi and IoT devices.

Wi-Fi and IoT devices of downlink transmission. It contains the address of the AP and selected Wi-Fi and IoT devices. (ii) Upon receipt of the NDPA packet, each of the Wi-Fi and IoT devices responds with an NDP packet immediately. This legacy NDP packet serves two purposes: confirming participation of a device in this round of transmission and providing reference signals for the AP to construct beamforming filters. (iii) Using the constructed beamforming filters, the AP sends packets to all Wi-Fi/IoT devices. (iv) After receiving the data packets, each device sends an ACK/NACK packet to the AP.

Beamforming at AP. In this protocol, we need to figure out how to construct the precoding filters for beamforming at the AP so that each Wi-Fi/IoT device can successfully decode its desired signal. We take advantage of wireless channel reciprocity by directly using the decoding filters in the uplink as the beamforming filters in the downlink. Given that the uplink and downlink channels are reciprocal, if a set of spatial filters can support interference-free data transmission in the uplink, they can also support interference-free data transmission in the downlink.

Guided by this idea, we construct the beamforming filters as follows: First, the AP constructs the decoding filters for the Wi-Fi devices using (1) and for the IoT devices using (2) by leveraging the reference signals in the uplink NDP packets as shown in Fig. 8. Then, it directly uses constructed decoding filters to precode the downlink signals for both Wi-Fi and IoT devices. Mathematically, the AP precodes its downlink signals as follows:

$$\mathbf{S}(l,k) = \sum_{i=1}^{W} \mathbf{G}_i(k)^* S_i(l,k) + \mathbf{G}(k)^* S(l,k), \qquad (3)$$

where $S_i(l,k)$ is the data that the AP wants to send to Wi-Fi device i on subcarrier k in OFDM symbol l; $S(l,k)$ is the data that the AP wants to send to IoT device k in data symbol l; $\mathbf{S}(l,k)$ is the precoded baseband signal vector that the AP sends to its M antenna ports on subcarrier k in OFDM symbol l; $\mathbf{G}_i(k)$ and $\mathbf{G}(k)$ are calculated at the AP using (1) and (2) by leveraging the uplink sounding signals in the protocol.

Channel Calibration: In real systems, although over-the-air channels are reciprocal, the Tx and Rx RF circuits are not. To maintain the reciprocity of compound uplink and downlink channels, we employ the relative calibration method in [32]. This relative calibration method is an internal and standalone calibration method that can be done at the AP without requiring involvement of user devices. In our experiments, we implement this calibration method to maintain the channel reciprocity.

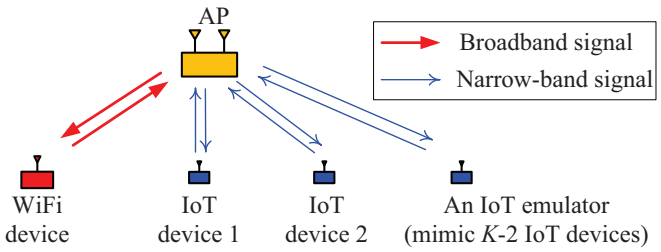

Fig. 9: A prototyped WiFi-IoT system that comprises a two-antenna AP, a Wi-Fi device, two IoT devices, and an IoT emulator. The IoT emulator is used to mimic $(K-2)$ IoT devices for ease of implementation, $K \in \{12, 16, 24\}$.

D. Discussions

The heterogeneous MU-MIMO uplink and downlink protocols, along with the proposed signal detection and beamforming methods, constitute the coexistence scheme that enables the Wi-Fi and IoT devices to share the spectrum simultaneously. We have the following remarks on the proposed coexistence scheme.

Remark 1. For both the signal detection method in the uplink and the beamforming method in the downlink, it is hard to analytically quantify their performance. Therefore, we resort to experiments to show their performance in real-world wireless environments.

Remark 2. In the proposed coexistence scheme, neither the signal detection nor the beamforming method requires CSI. Instead, they use the reference signals in the frame to construct the decoding/beamforming filters directly. As the channel estimation in conventional wireless networks typically incurs a large amount of airtime overhead, the removal of channel estimation in the proposed coexistence scheme not only improves the spectral efficiency but also reduces the implementation complexity.

Remark 3. The two MAC protocols are lightweight. The signal detection and beamforming methods have a low computational complexity. Therefore, the proposed coexistence scheme is amenable to practical implementation.

V. Experimental Evaluation

In this section, we conduct experiments in real-world wireless environments to evaluate the performance of WiFi-IoT in both uplink and downlink data transmissions.

A. System Implementation

We have built a prototype of WiFi-IoT in the network as shown in Fig. 9, which comprises an AP, a Wi-Fi device, two independent IoT devices, and an IoT emulator. The AP has two antennas, and the Wi-Fi/IoT devices have a single antenna. The IoT emulator is used to mimic $(K-2)$ IoT devices when $K \in \{12, 16, 24\}$. The purpose of this device is to reduce

TABLE I: EVM specification in IEEE 802.11ac standards [31].

EVM (dB)	(inf -5)	[-5 -10)	[-10 -13)	[-13 -16)	[-16 -19)	[-19 -22)	[-22 -25)	[-25 -27)	[-27 -30)	[-30 -32)	[-32 -inf)
Modulation	N/A	BPSK	QPSK	QPSK	16QAM	16QAM	64QAM	64QAM	64QAM	256QAM	256QAM
Coding rate	N/A	1/2	1/2	3/4	1/2	3/4	2/3	3/4	5/6	3/4	5/6
γ(EVM)	0	0.5	1	1.5	2	3	4	4.5	5	6	20/3

the experimental complexity. The system has been built on a software-defined radio (SDR) wireless testbed that consists of USRP2 [33] and GNURadio software package [34]. C++ language has been used to implement all the signal processing and protocol modules in GNURadio.

PHY Implementation: The communications between the AP and the Wi-Fi device are conducted using the legacy IEEE 802.11 frame [31]. The baseband signal processing chains required for packet transmission and reception have been implemented on both the AP and the Wi-Fi device.

The communications between the AP and the IoT devices are conducted using the IoT frame in Fig. 4, with $M_p = 12$, $M_s = 50$, and $M_d = 50$. The total number of symbols in the IoT frame is set to 1044. The proposed baseband signal processing chains in Fig. 3a and Fig. 3b have been implemented on the AP and each IoT device for data packet transmission and reception.

At the AP, its sampling rate is set to 20 Msps, and its transmit power is set to 20 dBm. At the Wi-Fi device, its sampling rate is also set to 20 Msps, and its transmit power is set to 20 dBm as well. At the IoT devices, we use $4\times$ oversampling factor and thus set their sampling rate to 1 Msps. Since an IoT device uses a single subcarrier for packet transmission, we scale down its transmit power to $20 - 10\log_{10}(52/1) \approx 3$, where 20 (dBm) is Wi-Fi device's transmit power, 52 is the number of valid subcarriers used by Wi-Fi devices, and 3 (dBm) is an IoT device's transmit power. With this transmit power, an IoT device has a similar communication range as a Wi-Fi device.

MAC Implementation: We have implemented the proposed coexistence scheme on this WiFi-IoT system. Specifically, we have implemented the MAC protocol in Fig. 7 as well as the proposed heterogeneous MU-MIMO detection algorithms to enable uplink data transmissions. We have also implemented the MAC protocol in Fig. 8 and the proposed beamforming algorithm as well as the relative channel calibration method in [32] to enable downlink data transmissions.

B. Experimental Setup and Performance Metrics

Experimental Setup: We measure the performance of the Wi-Fi and IoT communications in an office building as shown in Fig. 10. The AP is placed at the spot marked by "AP". Around the AP, we randomly picked up 32 locations and divided them into 8 groups. Each group has 4 locations (marked by the same symbol in Fig. 10), at which we placed the Wi-Fi device and the three IoT devices. Specifically, at location index i ($1 \le i \le 8$), the Wi-Fi device is placed at L_{i4}; the two IoT devices are placed at L_{i1} and L_{i2}; and the IoT emulator is placed at L_{i3}. In our experiments, we use the IoT device at L_{i1} as the representative when presenting the performance of IoT communications.

Performance Metrics: We use two performance metrics to assess the performance of the proposed WiFi-IoT solution.

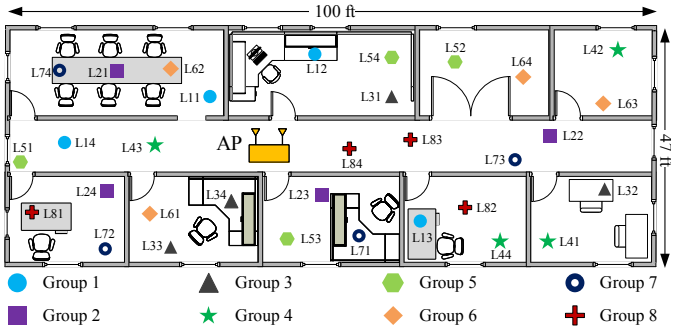

Fig. 10: The floor plan for performance evaluation.

The first one is error vector magnitude (EVM), which is widely used in wireless systems. EVM quantifies the normalized error magnitude between the measured constellation and the ideal constellation. Mathematically, it can be written as: $\text{EVM (dB)} = 10\log_{10}\left(\frac{\mathbb{E}(|x-\hat{x}|^2)}{\mathbb{E}(|x|^2)}\right)$, where x is the original signal at the transmitter and $\hat{x}$ is the estimated signal at the receiver.

The second performance metric that we use is data rate. Different from EVM, which is directly measured from the experimentation, the data rate is extrapolated based on the modulation and coding scheme (MCS) table specified in IEEE 802.11 standard as shown in Table I. Specifically, for the Wi-Fi device, its uplink/downlink data rate is calculated by: $r = \frac{48}{80} \times 20 \times \gamma(\text{EVM})$ Mbps, where 48 is the number of payload subcarriers, 80 is the points of one OFDM symbol (including CP), 20 is the Wi-Fi signal sampling rate (in Msps), and γ(EVM) is the average number of bits carried by one symbol and its possible values are given in Table I. For the IoT device, its uplink/downlink data rate is calculated by: $r = 250 \times \gamma(\text{EVM})$ kbps, where 250 is the IoT signal baud rate (in ksps) and γ(EVM) is given in Table I.

C. A Case Study

Before presenting the complete results, we first use a case study to examine the details of the proposed WiFi-IoT solution. In this case study, we placed the Wi-Fi and IoT devices at location index 1 (i.e., L_{11}, L_{12}, L_{13}, and L_{14}), and set the number of IoT devices to 12 (i.e., $K = 12$).

Uplink Results: In the uplink, the Wi-Fi and IoT devices send their packets to the AP simultaneously. The AP needs to decode both Wi-Fi and IoT signals. It is interesting to see the received power spectral density of the received Wi-Fi and IoT signals at the AP. Fig. 11(a-b) shows our experimental results. We can see that the received Wi-Fi signals have relatively flat spectrum, whereas the received IoT signals have 12 spectral peaks. Each spectral peak corresponds to one IoT device's signal. The bandwidth of the signal from one IoT device is about 250 kHz.

It is also interesting to see if the AP can successfully decode the concurrent Wi-Fi and IoT signals. Fig. 11(c) shows the

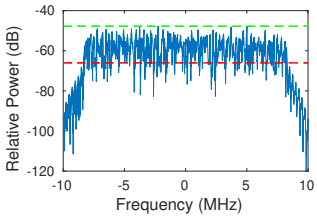

(a) Relative power spectral density of the received Wi-Fi signals at AP.

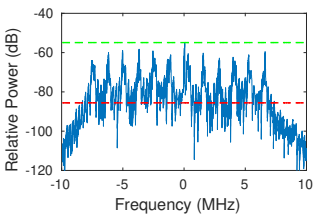

(b) Relative power spectral density of the received IoT signals at AP.

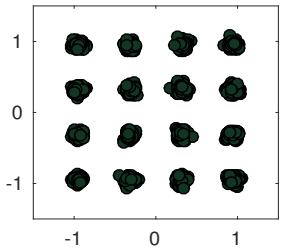

(c) Decoded Wi-Fi signals at AP.

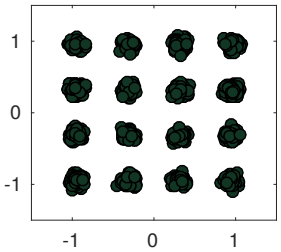

(d) Decoded IoT signals at AP.

Fig. 11: Uplink performance: (a-b) shows relative power spectral density of the Wi-Fi and IoT signals received by the AP's first antenna; (c-d) shows the constellation of decoded Wi-Fi and IoT signals at the AP when $K = 12$.

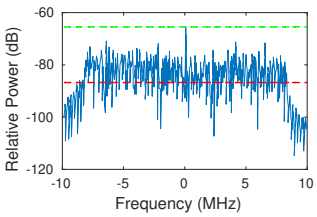

(a) Relative power spectral density of the received signals at the Wi-Fi device.

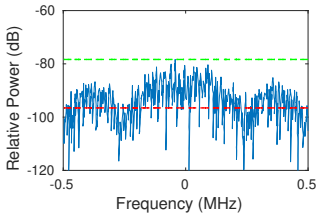

(b) Relative power spectral density of the received signals at one IoT device.

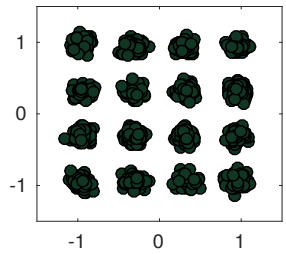

(c) Decoded signals at the Wi-Fi device.

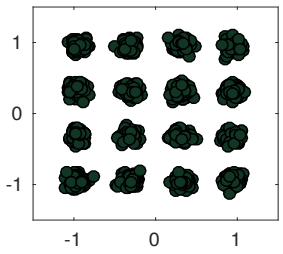

(d) Decoded signals at one IoT device.

Fig. 12: Downlink performance: (a-b) shows relative power spectral density of the received signals at the Wi-Fi device and one IoT device; (c-d) shows the constellation of decoded signals at the Wi-Fi device and one IoT device when $K = 12$.

constellation of the decoded Wi-Fi signals; Fig. 11(d) shows the constellation of the decoded IoT signals. It is evident that, using our proposed signal detection method, the AP can successfully decode both Wi-Fi and IoT signals. More specifically, our experimental results show that the EVM of the decoded Wi-Fi and IoT signals are -25.6 dB and -23.9 dB, respectively. This indicates that the AP can successfully serve the heterogeneous devices (one broadband Wi-Fi device and 12 narrow-band IoT devices) simultaneously.

Downlink Results: In the downlink, the AP performs beamforming to send data packets to the Wi-Fi and IoT devices simultaneously. Similar to the uplink, we examine the power spectral density and the decoded signals on the receiver side (the Wi-Fi and IoT devices) to see if the AP can successfully serve both Wi-Fi and IoT devices simultaneously.

Fig. 12(a) shows the power spectral density of the received signals at the Wi-Fi device; Fig. 12(b) shows the power spectral density of the received signals at one IoT device. Fig. 12(c) shows the constellation of the decoded signals at the Wi-Fi device and Fig. 12(d) shows the constellation of the decoded signals at one IoT device. It is evident that both devices can successfully decode their desired signals. The measured EVM is -21.5 dB at the Wi-Fi device and -22.0 dB at the IoT device.

Scrutinizing Beamforming in Downlink: Since the proposed beamforming method plays a critical role in the downlink transmission, we would like to further scrutinize the experimental results to examine its performance. Specifically, we would like to see the effectiveness of the proposed beamforming filters in the mitigation of inter-user interference.

We first examine the effectiveness of Wi-Fi beamforming filter (1). To do so, we first let the AP only transmit Wi-Fi signal (by setting the IoT signal to zero), and then observe the received signal at the Wi-Fi and IoT devices when two different beamforming filters are used. Fig. 13 exhibits our experimental results. By comparing Fig. 13(a) with Fig. 13(c), we can see that the Wi-Fi device can receive Wi-Fi signals with similar strength when the AP uses those two beamforming filters. By comparing Fig. 13(b) with Fig. 13(d), we can see that the proposed Wi-Fi beamforming filter can effectively mitigate the inter-user interference for the IoT devices. Compared to the equal-power beamforming, our proposed beamforming filters have more than 20 dB cancellation capability for inter-user interference.

We now examine the effectiveness of IoT beamforming filter (2) in the downlink. Similarly, we first let the AP only transmit IoT signal (by setting the Wi-Fi signal to zero), and then observe the received signal at the Wi-Fi and IoT devices when two different beamforming filters are used. Fig. 14 exhibits our experimental results. By comparing Fig. 14(b) with Fig. 14(d), we can see that the proposed IoT beamforming filters can effectively mitigate the inter-user interference for the Wi-Fi device. It has more than 15 dB cancellation capability for inter-user interference.

D. Complete Experimental Results

We now present all the measured experimental results from the 8 different locations in Fig. 10. Again, we use one IoT device (the one placed at L_{i1}, $1 \leq i \leq 8$) as the representative when presenting the performance of IoT communication.

Uplink Results: We collect the experimental data at the AP during the uplink communications. Fig. 15(a-b) presents the measured EVM of the decoded Wi-Fi and IoT signals at the

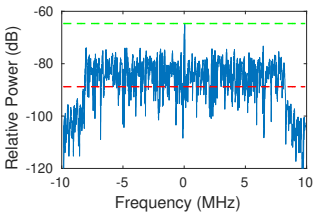

(a) Received signal at the Wi-Fi device when the AP uses beamforming filter (1).

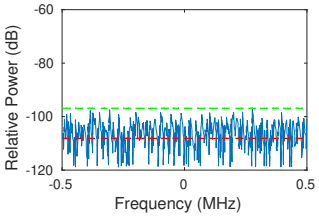

(b) Received signal at the IoT device when the AP uses beamforming filter (1).

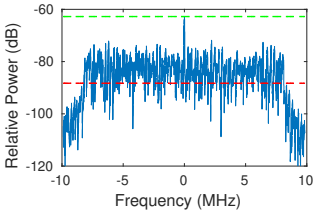

(c) Received signal at the Wi-Fi device when the AP uses beamforming filter $[\frac{1}{\sqrt{2}}\ \frac{1}{\sqrt{2}}]^T$.

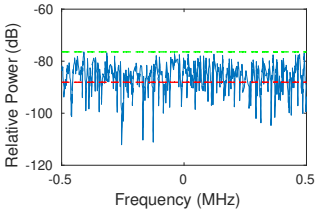

(d) Received signal at the IoT device when the AP uses beamforming filter $[\frac{1}{\sqrt{2}}\ \frac{1}{\sqrt{2}}]^T$.

Fig. 13: Relative power spectral density of the received signals at the Wi-Fi and IoT devices in the downlink when the AP sends Wi-Fi signals only.

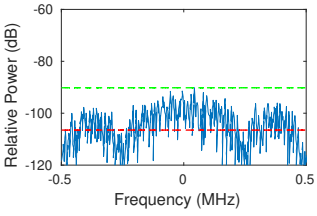

(a) Received signal at the IoT device when the AP uses beamforming filter (2).

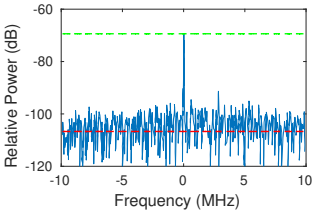

(b) Received signal at the Wi-Fi device when the AP uses beamforming filter (2).

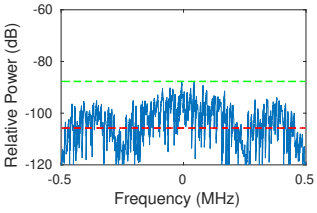

(c) Received signal at the IoT device when the AP uses beamforming filter $[\frac{1}{\sqrt{2}}\ \frac{1}{\sqrt{2}}]^T$.

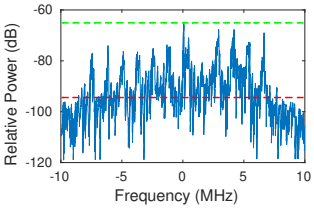

(d) Received signal at the Wi-Fi device when the AP uses beamforming filter $[\frac{1}{\sqrt{2}}\ \frac{1}{\sqrt{2}}]^T$.

Fig. 14: Relative power spectral density of the received signals at the Wi-Fi and IoT devices in the downlink when the AP only sends IoT signals.

AP. We can see that the EVM of the decoded Wi-Fi signals is less than -25.7 dB when there is no IoT device in the network ($K = 0$), less than -24.4 dB when $K = 1$, less than -22.0 dB when $K = 12$, less than -21.6 dB when $K = 16$, and less than -19.8 dB when $K = 24$. The EVM of the decoded IoT signals is less than -21.3 dB when $K = 1$, less than -18.6 dB when $K = 12$, less than -18.3 dB when $K = 16$, and less than -15.0 dB when $K = 24$. Meanwhile, we can see that the EVM of the decoded Wi-Fi and IoT signals slightly degrades as K increases. This is mainly because the inter-subcarrier interference becomes more significant as K increases.

Fig. 15(c) presents the extrapolated data rate of the uplink Wi-Fi communication. The achievable uplink data rate at the Wi-Fi device is greater than 54 Mbps when $K = 0$, greater than 48 Mbps when $K = 1$, greater than 48 Mbps when $K = 12$, greater than 36 Mbps when $K = 16$, and greater than 36 Mbps when $K = 24$. The increase of IoT devices slightly degrades the data rate of Wi-Fi communications. This is what we expected, and the degradation is attributed to the interference from the IoT devices. Fig. 15(d) presents the extrapolated data rate of the uplink IoT communication. The achievable uplink data rate at one IoT device is greater than 750 kbps when $K = 1$, greater than 500 kbps when $K = 12$, greater than 500 kbps when $K = 16$, and greater than 375 kbps when $K = 24$. The extrapolated data rate is more than sufficient for most existing and future IoT applications.

Downlink Results: We present the experimental data collected at the Wi-Fi and IoT devices during the downlink communications. Fig. 16(a-b) presents the measured EVM of the decoded signals at the Wi-Fi and IoT devices. We can see that the EVM of the decoded Wi-Fi signals is less than -25.2 dB when $K = 0$, less than -22.9 dB when $K = 1$, less than -18.6 dB when $K = 12$, less than -17.3 dB when $K = 16$, and less

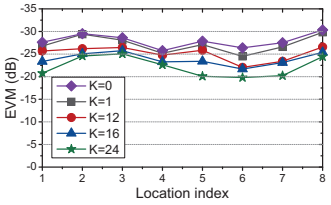

(a) Measured EVM of decoded Wi-Fi signal at the AP.

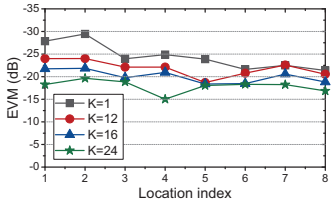

(b) Measured EVM of decoded IoT signal at the AP.

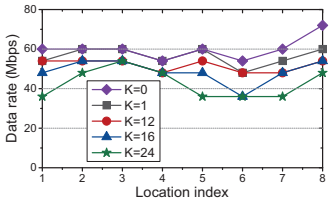

(c) Extrapolated data rate of uplink Wi-Fi communication.

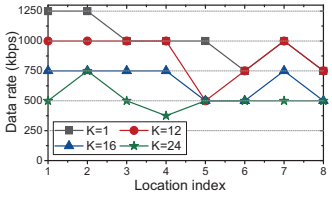

(d) Extrapolated data rate of uplink IoT communication.

Fig. 15: Measured EVM and extrapolated data rate in the uplink communication.

than -15.4 dB when $K = 24$. The EVM of the decoded IoT signals is less than -22.4 dB when $K = 1$, less than -19.3 dB when $K = 12$, less than -18.2 dB when $K = 16$, and less than -14.6 dB when $K = 24$. Similar to the uplink, the EVM measured in the downlink slightly degrades as K increases. This is also because the interference leakage becomes more significant as K increases.

Fig. 16(c) presents the extrapolated data rate of the uplink Wi-Fi communication. The achievable downlink data rate at the Wi-Fi device is greater than 54 Mbps when $K = 0$, greater than 48 Mbps when $K = 1$, greater than 24 Mbps when $K = 12$, greater than 24 Mbps when $K = 16$, and greater than 18 Mbps when $K = 24$. Fig. 16(d) presents the

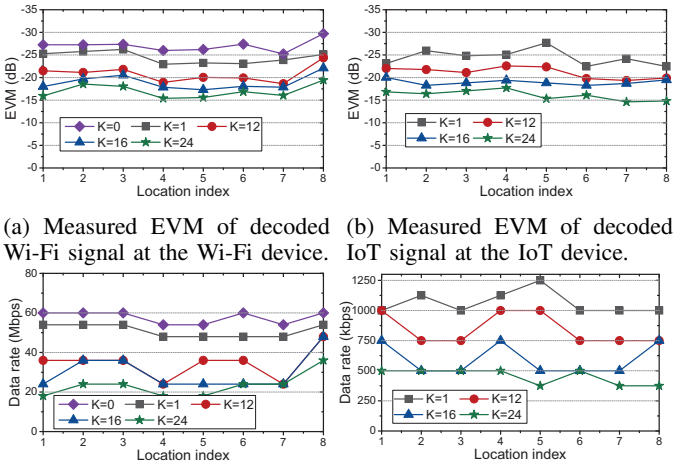

(a) Measured EVM of decoded Wi-Fi signal at the Wi-Fi device.

(b) Measured EVM of decoded IoT signal at the IoT device.

(c) Extrapolated data rate of downlink Wi-Fi communication.

(d) Extrapolated data rate of downlink IoT communication.

Fig. 16: Measured EVM and extrapolated data rate in the downlink communication.

extrapolated data rate of the uplink IoT communication. The achievable downlink data rate at one IoT device is greater than 1000 kbps when $K = 1$, greater than 750 kbps when $K = 12$, greater than 500 kbps when $K = 16$, and greater than 375 kbps when $K = 24$. The achieved data rate for Wi-Fi and IoT communications meets the requirements of most Wi-Fi and IoT applications.

E. Summary of Observations

Based on the above experimental results, we have the following observations: First, a non-OFDM IoT device can communicate with an OFDM-based AP using a low sampling rate (250 ksps or 1 Msps). Second, in a typical office building, an AP with two antennas can serve one Wi-Fi device and 24 IoT devices simultaneously in both downlink and uplink. Third, the Wi-Fi device can achieve more than 36 Mbps in the uplink and more than 24 Mbps in the downlink. Fourth, the IoT device can achieve more than 375 kbps in both uplink and downlink.

VI. Conclusion

In this paper, we proposed WiFi-IoT, an energy-efficient IoT communication solution for future Wi-Fi networks. WiFi-IoT features two innovative techniques. The first one is an asymmetric PHY design, which allows an OFDM-based AP to communicate with multiple QAM-based (non-OFDM) IoT devices simultaneously. Such an asymmetric PHY makes it possible for the IoT devices to transmit/receive their signals at a low sampling rate (250 ksps), thereby conserving their power consumption for radio communications. The second one is a transparent coexistence scheme, which enables an AP with multiple antennas to serve broadband Wi-Fi devices and narrow-band IoT devices simultaneously. We have built a prototype of WiFi-IoT on a wireless testbed and evaluated its performance in real-world wireless environments. Experimental results show that, using the proposed WiFi-IoT solution, a two-antenna AP can communicate with one legacy Wi-Fi device and 24 narrow-band IoT devices simultaneously in both uplink and downlink.

References

[1] C.-L. Hsu and J. C.-C. Lin, "An empirical examination of consumer adoption of Internet of Things services: Network externalities and concern for information privacy perspectives," *Computers in Human Behavior*, vol. 62, pp. 516–527, 2016.

[2] A. Zanella, N. Bui, A. Castellani, L. Vangelista, and M. Zorzi, "Internet of Things for smart cities," *IEEE Internet of Things journal*, vol. 1, no. 1, pp. 22–32, 2014.

[3] B. L. R. Stojkoska and K. V. Trivodaliev, "A review of Internet of Things for smart home: Challenges and solutions," *Journal of Cleaner Production*, vol. 140, pp. 1454–1464, 2017.

[4] J. J. Rodrigues, D. B. D. R. Segundo, H. A. Junqueira, M. H. Sabino, R. M. Prince, J. Al-Muhtadi, and V. H. C. De Albuquerque, "Enabling technologies for the Internet of health things," *IEEE Access*, vol. 6, pp. 13129–13141, 2018.

[5] L. Da Xu, W. He, and S. Li, "Internet of Things in industries: A survey," *IEEE Transactions on industrial informatics*, vol. 10, no. 4, pp. 2233–2243, 2014.

[6] J. A. Guerrero-Ibanez, S. Zeadally, and J. Contreras-Castillo, "Integration challenges of intelligent transportation systems with connected vehicle, cloud computing, and Internet of Things technologies," *IEEE Wireless Communications*, vol. 22, no. 6, pp. 122–128, 2015.

[7] S. Farahani, *ZigBee wireless networks and transceivers*. Amsterdam, The Netherlands: Newnes, 2011.

[8] M. Bouaziz and A. Rachedi, "A survey on mobility management protocols in wireless sensor networks based on 6LoWPAN technology," *Computer Communications*, vol. 74, pp. 3–15, 2016.

[9] A. F. Harris III, V. Khanna, G. Tuncay, R. Want, and R. Kravets, "Bluetooth low energy in dense IoT environments," *IEEE Communications Magazine*, vol. 54, no. 12, pp. 30–36, 2016.

[10] M. B. Yassein, W. Mardini, and A. Khalil, "Smart homes automation using Z-Wave protocol," in *IEEE International Conference on Engineering & MIS (ICEMIS)*, pp. 1–6, 2016.

[11] Qualcomm Technologies, Inc., "Narrowband IoT (NB-IoT)." RP-151621, 3GPP TSG RAN Meeting #69, September 2015.

[12] Texas Instruments, "Analog-to-digital converters (ADCs)-products," *www.ti.com/data-converters/adc-circuit/products.html [Online; Accessed: 2019-04-12]*.

[13] K. Maharatna, E. Grass, and U. Jagdhold, "A 64-point Fourier transform chip for high-speed wireless LAN application using OFDM," *IEEE Journal of Solid-State Circuit*, vol. 39, no. 3, pp. 484–493, 2004.

[14] J. Jensen, R. Sadhwani, A. Kidwai, B. Jann, A. Oster, M. Sharkansky, I. Ben-Bassat, O. Degani, S. Porat, A. Fridman, *et al.*, "Single-chip WiFi b/g/n 1× 2 SoC with fully integrated front-end & PMU in 90nm digital CMOS technology," in *2010 IEEE Radio Frequency Integrated Circuits Symposium*, pp. 447–450, 2010.

[15] 3GPP TR 45.820, "Cellular system support for ultra low complexity and low throughput Internet of Things." V2.1.0, August 2015.

[16] Ericsson and N. Networks, "Further LTE physical layer enhancements for MTC." RP-141660, 3GPP TSG RAN Meeting #65, September 2014.

[17] J. Xu, J. Yao, L. Wang, Z. Ming, K. Wu, and L. Chen, "Narrowband Internet of Things: Evolutions, technologies, and open issues," *IEEE Internet of Things Journal*, vol. 5, no. 3, pp. 1449–1462, 2017.

[18] "IEEE Standard for Information technology–Telecommunications and information exchange between systems - Local and metropolitan area networks–Specific requirements - Part 11: Wireless LAN Medium Access Control (MAC) and Physical Layer (PHY) Specifications Amendment 2: Sub 1 GHz License Exempt Operation," *IEEE Std 802.11ah-2016 (Amendment to IEEE Std 802.11-2016, as amended by IEEE Std 802.11ai-2016)*, pp. 1–594, May 2017.

[19] B. Bellalta, "IEEE 802.11ax: High-efficiency WLANs," *IEEE Wireless Communications*, vol. 23, no. 1, pp. 38–46, 2016.

[20] N. Butt, R. Di Taranto, D. Sundman, and L. Wilhelmsson, "On the feasibility to overlay a narrowband IoT signal in IEEE 802.11," in *IEEE 28th Annual International Symposium on Personal, Indoor, and Mobile Radio Communications (PIMRC)*, pp. 1–7, 2017.

[21] Y. Wang, L. F. Del Carpio, D. Sundman, D. Peddireddy, and A. Larmo, "MAC layer design and evaluation of a narrowband Wi-Fi system," in *IEEE 28th Annual International Symposium on Personal, Indoor, and Mobile Radio Communications (PIMRC)*, pp. 1–6, 2017.

[22] L. R. Wilhelmsson, M. M. Lopez, and D. Sundman, "NB-WiFi: IEEE 802.11 and Bluetooth low energy combined for efficient support of IoT," in *IEEE Wireless Communications and Networking Conference (WCNC)*, pp. 1–6, 2017.

[23] T. Yucek and H. Arslan, "A survey of spectrum sensing algorithms for cognitive radio applications," *IEEE communications surveys & tutorials*, vol. 11, no. 1, pp. 116–130, 2009.

[24] D. Yang, Y. Xu, and M. Gidlund, "Wireless coexistence between IEEE 802.11-and IEEE 802.15.4-based networks: A survey," *International Journal of Distributed Sensor Networks*, vol. 7, no. 1, p. 912152, 2011.

[25] Q. Zhao and B. M. Sadler, "A survey of dynamic spectrum access," *IEEE signal processing magazine*, vol. 24, no. 3, pp. 79–89, 2007.

[26] H. Pirayesh, P. Kheirkhah Sangdeh, and H. Zeng, "EE-IoT: An energy-efficient IoT communication scheme for WLANs," in *IEEE INFOCOM 2019*, pp. 361–369, 2019.

[27] P. Kheirkhah Sangdeh, H. Pirayesh, H. Zeng, and H. Li, "A practical underlay spectrum sharing scheme for cognitive radio networks," in *IEEE INFOCOM*, pp. 2521–2529, IEEE, 2019.

[28] H. Zeng, C. Cao, H. Li, and Q. Yan, "Enabling jamming-resistant communications in wireless MIMO networks," in *IEEE Conference on Communications and Network Security (CNS)*, 2017.

[29] Q. Yan, H. Zeng, T. Jiang, M. Li, W. Lou, and Y. T. Hou, "Jamming resilient communication using MIMO interference cancellation," *IEEE Transactions on Information Forensics and Security*, vol. 11, no. 7, pp. 1486–1499, 2016.

[30] Q. Yan, H. Zeng, T. Jiang, M. Li, W. Lou, and Y. T. Hou, "MIMO-based jamming resilient communication in wireless networks," in *IEEE INFOCOM*, pp. 2697–2706, 2014.

[31] IEEE 802.11ac, "IEEE standard for information technology local and metropolitan area networks part 11: Wireless LAN medium access control (MAC) and physical layer (PHY) specifications amendment 5: Enhancements for higher throughput," *IEEE Standards 802.11ac*, 2014.

[32] C. Shepard, H. Yu, N. Anand, E. Li, T. Marzetta, R. Yang, and L. Zhong, "Argos: Practical many-antenna base stations," in *ACM 18th annual international conference on Mobile computing and networking*, pp. 53–64, 2012.

[33] Ettus Research, "USRP N210," *www.ettus.com/product/details/UN210-KIT [Online; Accessed 8-March-2018]*.

[34] "A free and open-source toolkit for software radio," *http://gnuradio.org [Online; Accessed 23-May-2019]*.